Figure S1-related to Figure 1

A

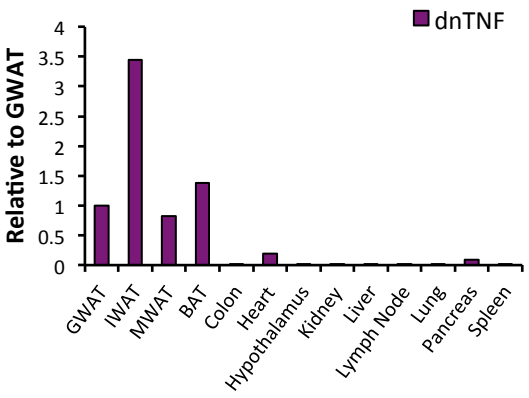

B

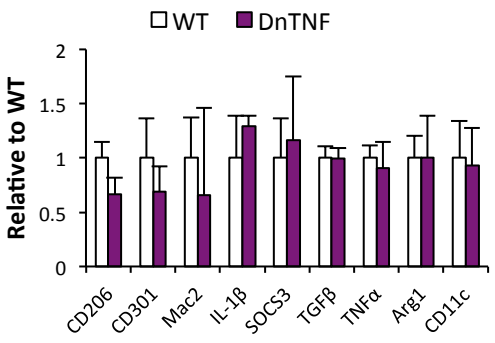

C

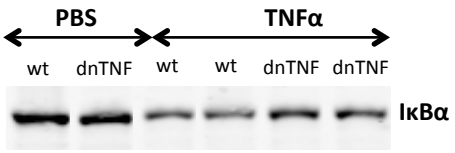

D

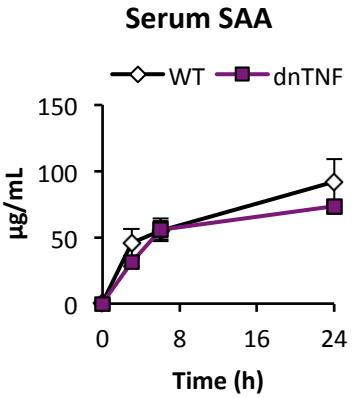

E

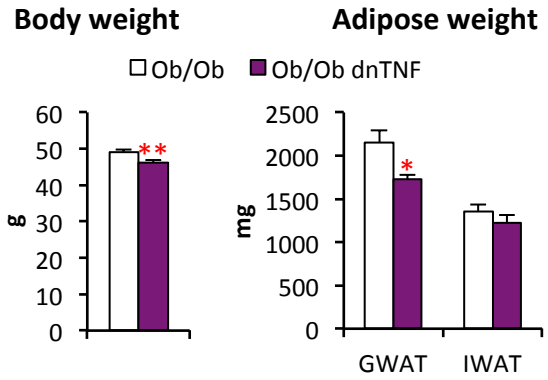

Figure S2-related to Figure 2

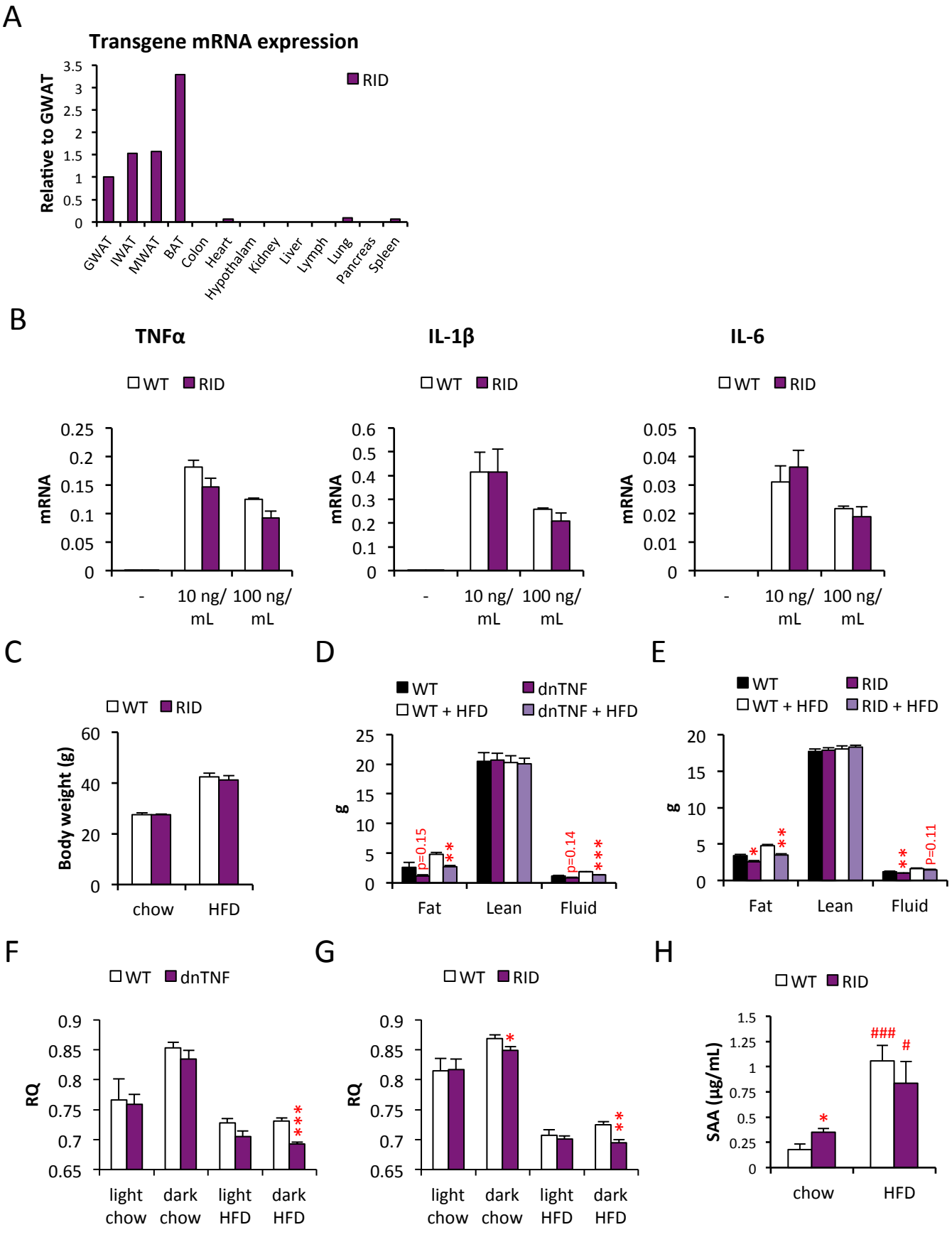

Figure S3-related to Figure 3

A

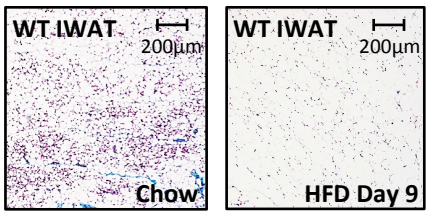

B

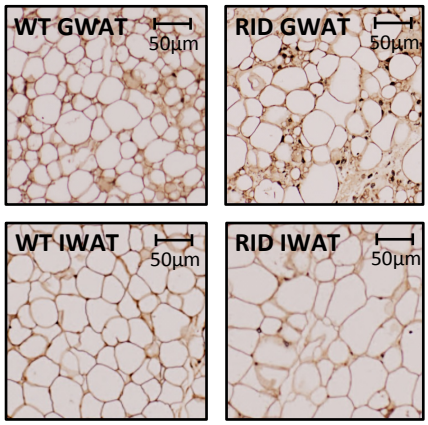

C

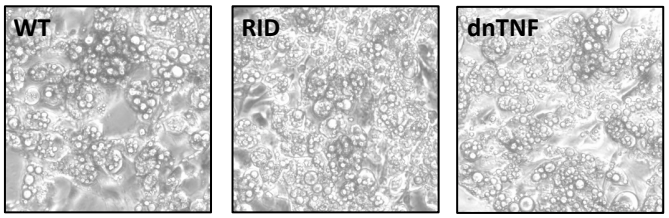

D

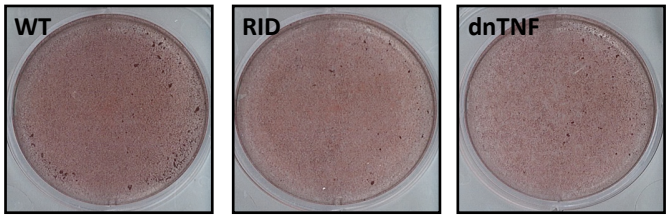

E

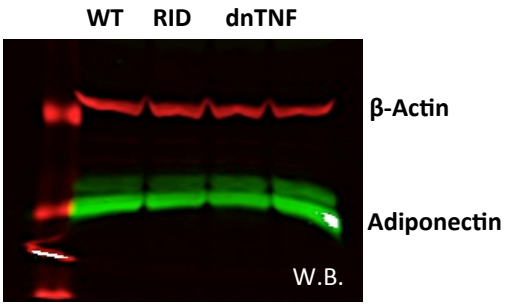

Figure S4-Related to Figure 4

A

Hypothesis:
Effects of microbiota-induced inflammation on adipogenesis during development.

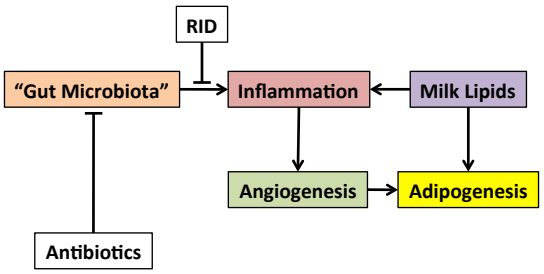

B

Hypothesis:
Effects of microbiota-induced inflammation on adipogenesis on MWAT in adulthood

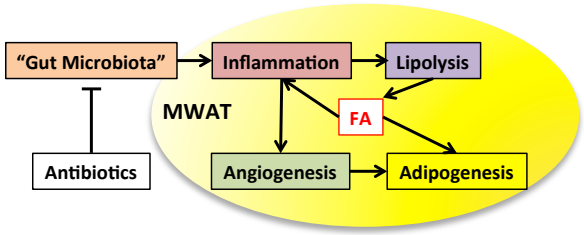

C

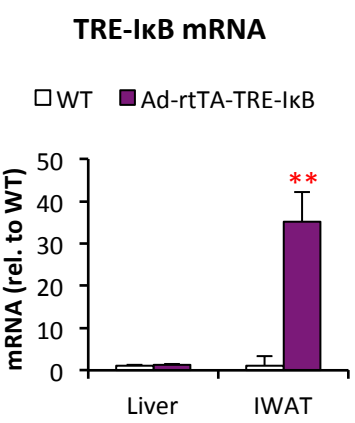

D

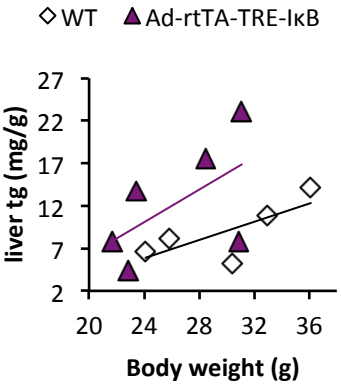

Figure S5-Related to Figure 5

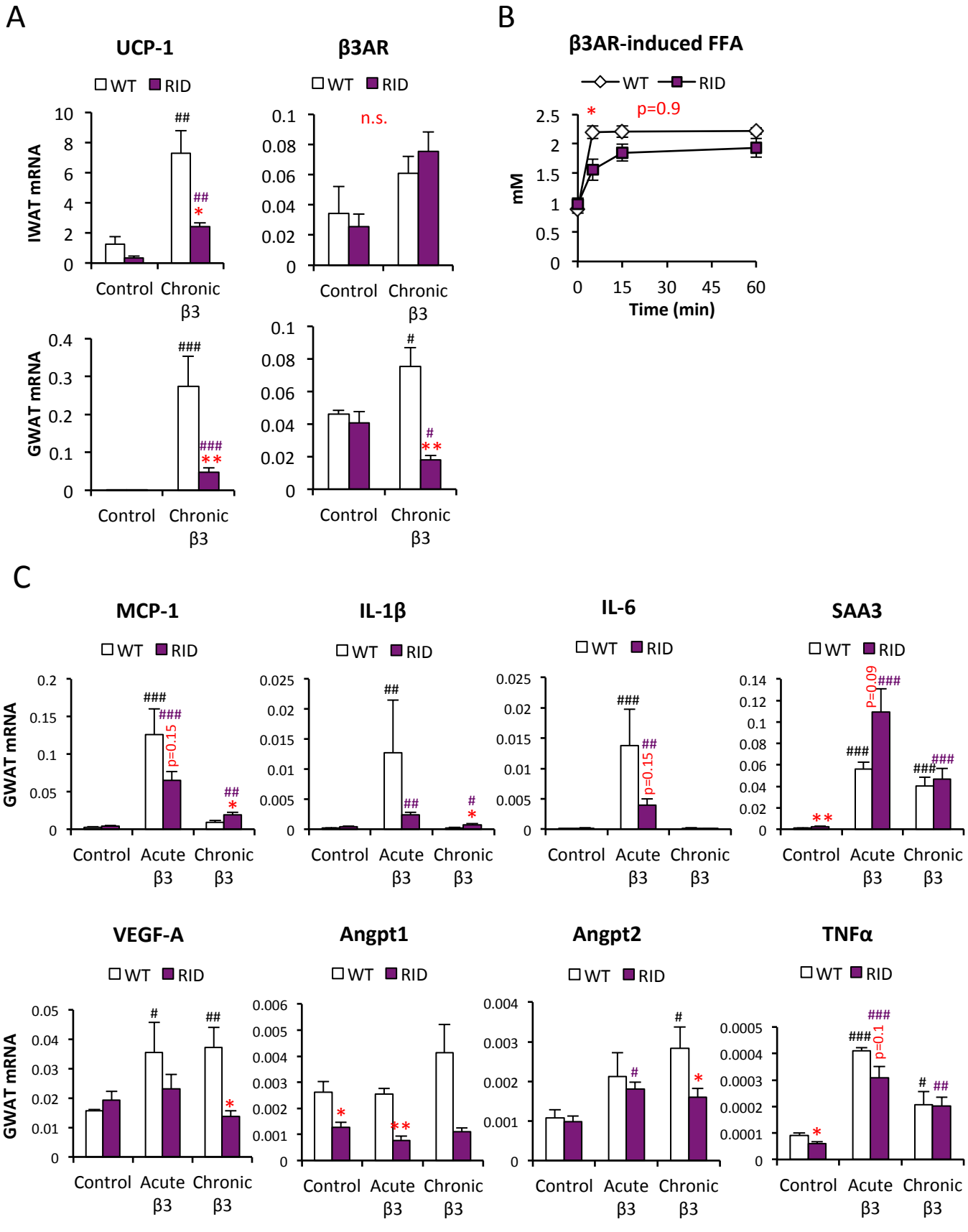

Figure S6-Related to Figure 6

A

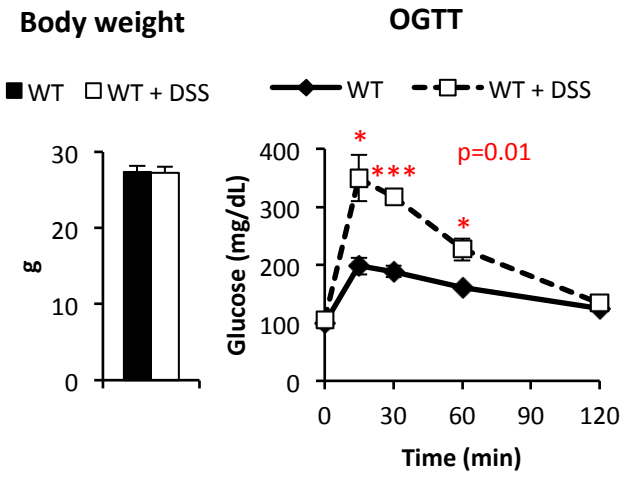

B

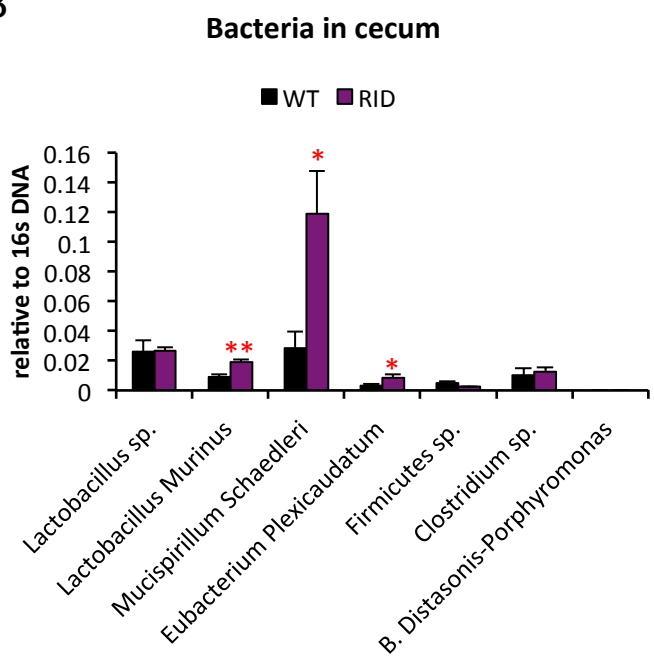

Supplemental Figure Legends

Figure S1, related to Figure 1. (A) dnTNF transgene mRNA expression (B) Gene expression analysis of isolated macrophages from dnTNF tg an littermate control mice (C) Description of the dnTNF tg mouse model (top) and NFkB activation in GWAT harvested from dnTNF tg and wildtype females 1h post TNFα or vehicle injection i.p. (D) SAA-levels in dnTNF tg mice after i.p. injection with 0.3 mg/kg LPS in dnTNF tg and wildtype female mice. (E) Body weight and dissected fat pad weights in dnTNF tg Ob/Ob mice and littermate Ob/Ob control mice. Error bars represent SEM, a p-value <0.05 according to student t-test was considered as significant and is indicated by *; **: p<0.01; ***: p<0.001 for differences between genotypes.

Figure S2, related to Figure 2. (A) RID transgene mRNA expression (B) Gene expression analysis of isolated peritoneal macrophages, treated with or without LPS, from RID tg and wildtype control mice. (C) Body weight in male RID tg and wildtype mice. Body composition analyses of (D) dnTNF and (E) RID tg mice on chow and after 2 days with HFD. RQ (VO_2/VCO_2) measurements over a 4-day period in (F) dnTNF and (G) RID tg mice on chow day 1-2 and HFD day 3-4. (H) Serum SAA levels in chow-fed and 15-weeks HFD fed RID tg and wild type mice. 1-way ANOVA analysis shows that diet (F=8.8, p=0.01) but not genotype (F=0.3, p=0.5) contribute significantly to SAA levels. Error bars represent SEM, a p-value <0.05 according to student t-test was considered as significant and is indicated by *; **: p<0.01; ***: p<0.001 for differences between genotypes.

Figure S3, related to Figure 3. (A) Representative Trichrome stain of IWAT from 8-week old C57B6 males on chow and after 9 day with HFD. (B) Representative perilipin stain of GWAT and IWAT from 10-day old male RID tg and wildtype pups. (C) Bright field micrograph, (D) Oil-Red O stain and (E) intracellular adiponectin levels of differentiated adipocytes from stromal-vascular fraction isolated from WT, RID tg and dnTNF tg IWAT.

Figure S4, related to Figure 4. (A-B) Drawings depict hypotheses of the effects of gut microbiota-induced inflammation on adipogenesis during postnatal development (A) and on MWAT in adult mice (B). (C) Iκb mRNA levels in IWAT and liver in doxycycline-treated Ad-rtTA-TRE-IκB tg and littermate controls. (D) Liver triglyceride (tg) content in relation to body weight in HFD-fed Ad-rtTA-TRE-IκB tg male mice. Error bars represent SEM, a p-value <0.05 according to student t-test was considered as significant and is indicated by *; **: p<0.01; ***: p<0.001 for differences between genotypes.

Figure S5, related to Figure 5. (A) IWAT and GWAT expression of β_3AR and UCP-1 mRNA at baseline and after chronic β_3AR-agonist treatment in male RID tg and wildtype mice. (B) FFA-levels in response to β_3AR-agonist injection in male RID tg and wildtype mice. (C) Gene expression analyses of GWAT 3 h (acute) after β_3AR-agonist injection and after chronic treatment (IWAT harvested 24 h after last injection) in male RID tg and wildtype mice. Error bars represent SEM and a p-value <0.05 according to student t-test

was considered as significant and is indicated by */#; **/##: p<0.01; ***/###: p<0.001 (*significantly different from WT, # significantly different from untreated controls of same genotype). P-value in red indicates the difference between groups during the entire time course according to repeated measurement ANOVA. Additional 1-way ANOVA analyses have been performed for Supplemental Figure 4G (**Table S3**)

Figure S6, related to Figure 6. (A) Body weight and glucose tolerance test in 5 day DSS-treated (2% in drinking water) and control FVB male mice. (B) Analysis of bacterial composition in cecal content harvested from RID tg and wildtype mice. Error bars represent SEM and a p-value <0.05 according to student t-test was considered as significant and is indicated by *; **: p<0.01; ***: p<0.001 for differences between groups/genotypes. P-value in red indicates the difference between groups during the entire time course according to repeated measurement ANOVA.

Table S1, related to Figure 7. Mouse phenotype summary

	dnTNF tg	RID tg	Ad-rtTA-TRE-IκB tg
Body weight (unchallenged)	(↓)	→	→
IWAT weight (unchallenged)	↓	↓	↓
GWAT weight (unchallenged)	→	↓	→
MWAT weight (unchallenged)	→	↓	→
BAT weight (unchallenged & HFD)	→	→	→
HFD-induced weight gain	↓	→	→
HFD-induced GWAT expansion (mg/g)	↓	↓	↓
HFD-induced MWAT expansion (mg/g)	→	↓	→
HFD-induced IWAT expansion (mg/g)	→	→	→
Postnatal IWAT expansion	↓	↓	↓
Oxygen consumption	→	→	NA
Food intake	→	→	NA
RER (dark phase)	↓	↓	NA
RER (light phase)	→	→	NA
ECM in adipose tissue (HFD)	↑	↑	NA
Serum Adiponectin levels (HFD)	↓	↓	NA
Serum SAA levels (chow)	(↓)	↑	NA
Serum SAA levels (HFD)	↓	→	NA
Capillary density in adipose tissue	NA	↓	NA
Glucose tolerance (unchallenged)	→	↓	→
Glucose tolerance (HFD)	↓	↓	↓
Liver weight (HFD, mg/g)	→	↑	↑
HFD-induced hepatic steatosis	↑	↑	(↑)
β3AR-agonist induced “browning” of WAT	NA	↓	NA
Colon hyperplasia	→	↑	→
Spleen weight (unchallenged)	→	↑	→
Liver weight (unchallenged)	→	↑	→
Intestinal permeability	NA	↑	NA
Colitis	NA	↑	NA
Altered gut microbiota	NA	yes	NA

Arrows in parenthesis indicated non-significant trends

Table S2, related to experimental procedures. Primer sequences

GENE	FORWARD PRIMER	REVERSE PRIMER
β-Actin	5'-GACCCAGATCATGTTTGAGA-3'	5'-GAGCATAGCCCTCGTAGAT-3'
SAA1	5'-ACACCAGGATGAAGCTACTCACCA-3'	5'-CCCTTGGAAAGCCTCGTGAACAAA-3'
SAA2	5'-AGCTGGCTGGAAAGATGGAGACAA-3'	5'-TGTCCTCTGCCGAAGAATTCCTGA-3'
SAA3	5'-TAAAGTCATCAGCGATGCCAGAG-3'	5'-CAACCCAGTAGTTGCTCCTCTTC-3'
F4/80	5'-CTTTGGCTATGGGCTTCCAGTC-3'	5'-GCAAGGAGGACAGAGTTTATCGTG-3'
VEGF-A	5'- GGAGATCCTTCGAGGAGCACTT	5'- GGCGATTTAGCAGCAGATATAAGAA
MPO	5'-CACCCTCTTTGTTCGAGAGC-3'	5'-CAACACCAAGGGCAGGTAGT-3'
MCP-1	5'-ACTGAAGCCAGCTCTCTCTTCC-3'	5'-TTCCTTCTTGGGGTCAGCACAG-3'
MIP1-α	5'-TGCCCTTGCTGTTCTTCTCT-3'	5'-CAGGCATTCAGTTCCAGGTC-3'
TNF	5′-GAGAAAGTCAACCTCCTCTCTG-3′	5′- GAAGACTCCTCCCAGGTATATG-3′
IL-1β	5'-CAACCAACAAGTGATATTCTCCATG-3'	5'-GATCCACACTCTCCAGCTGCA-3′
Angpt1	5'-CATTCTTCGCTGCCATTCTG-3'	5'-GCACATTGCCCATGTTGAATC-3′
Angpt2	5'-TTAGCACAAAGGATTCGGACAAT-3'	5'-TTTTGTGGGTAGTACTGTCCATTCA-3′
IL-6	5′- CCAGAGATACAAAGAAATGATGG-3'	5′- ACTCCAGAAGACCAGAGGAAAT-3′
UCP-1	5'-GTGAAGGTCAGAATGCAAGC-3'	5'-AGGGCCCCCTTCATGAGGTC-3′
β_3AR	5'-CCACTCCGGGAACACCG-3'	5'-GGCAGTAGATGACCGGGTTG-3′
TLR4	5'-GAATCCCTGCATAGAGGTAGTTCC-3'	5'-TGATCCATGCATTGGTAGGTAATATTA-3′
CD14	5'-ACTTCTAGATCCGAAGCCAG-3'	5'-CCGCCGTACAATTCCACAT-3′
IκB	5'-CAGCAGCTCACCGAGGAC-3'	5'-AAAGCCAGGTCTCCCTTCAC-3'

Table S3, related to Figure 5. Differences in gene expression in response to acute and chronic β3AR-agonist treatment in RID tg and wild type controls.

IWAT (Figure 5D)

	Fixed factors: GENOTYPE	**TREATMENT**	**WHOLE MODEL**
Dependent factor:	F-value; p-value	F-value; p-value	F-value; p-value
GENE EXPRESSION			
MCP-1	12.3; 0.002	27.3; <0.001	16.3; <0.001
IL-1β	4.5; 0.049	7.5; 0.005	4.9; 0.006
IL-6	1.6; 0.216	4.3; 0.029	2.8; 0.049
SAA3	3.2; 0.089	9.1; 0.002	5.1; 0.005
VEGF-A	13.0; <0.001	12.0; <0.001	8.6; <0.001
Angpt1	27.6; <0.001	3.3; 0.059	6.9; 0.001
Angpt2	5.1; 0.036	22.4; <0.001	10.5; <0.001
TNFα	0.5; 0.49	0.1; 0.916	0.3; 0.88

GWAT (Figure S5C)

	Fixed factors: GENOTYPE	**TREATMENT**	**WHOLE MODEL**
Dependent factor:	F-value; p-value	F-value; p-value	F-value; p-value
GENE EXPRESSION			
MCP-1	2.4; 0.142	28.1; <0.001	12.4; <0.001
IL-1β	0.64; 0.43	23.0; <0.001	10.6; <0.001
IL-6	3.5; 0.079	10.7; 0.001	5.6; 0.003
SAA3	5.2; 0.036	27.1; <0.001	14.2; <0.001
VEGF-A	6.2; 0.023	2.6; 0.107	3.54; 0.022
Angpt1	23.7; <0.001	1.8; 0.198	6.3; 0.002
Angpt2	3.5; 0.078	6.3; 0.009	3.8; 0.017
TNFα	3.0; 0.10	36.7; <0.001	15.1; <0.001

Supplemental Experimental Procedures

Generation of transgenic mice: Mutated human TNFα_A145R/Y87H, a dominant-negative form of TNFα (dnTNF) was amplified by PCR from a plasmid, kindly provided by Xencor Inc. A145R/Y87H is also referred to as XPro1595. XPro1595 as a recombinant protein can only exchange with and inactivate soluble TNFα (Zalevsky et al., 2007). However, when used as a transgene, dnTNF is co-expressed in the same cell as native TNF, and the dnTNF may form inactive trimers on the cell membrane, thereby also inhibiting transmembrane TNFα. A PCR product for dnTNF was purified and cloned into a TOPO TA Cloning® Kit (Invitrogen, USA) for entry into a Gateway vector containing the 5.4-kb aP2 enhancer/promoter sequence. The final construct was sequenced, linearized with Kpn1 and Drd1, and purified before pronuclear injection. Human dnTNFs, used as proteins, are able to heterotrimerize with and inactivate soluble mouse TNFα and block its activity *in vitro* and *in vivo* (Steed et al., 2003). The RIDα/β unit was amplified with PCR and excised from a vector containing the adenovirus E3 region (Delgado-Lopez and Horwitz, 2006), then sub-cloned into a pBluescript vector containing the 5.4-kb aP2 enhancer/promoter sequence using the EcoR1 and BamH1 restriction enzymes sites. The final RID-construct was sequenced, linearized with SalI and NotI, and purified before pronuclear injection.

Human IκBα (954 bp) was amplified from a cDNA library and engineered into pCR4TA vector (Invitrogen). The Ser32 and Ser36 residues were mutated to Gly and Ala respectively using a site-directed mutagenesis kit (Stratagene). The dominant negative mutant of IκBα was then subcloned into the pTet-on vector

(Clontech), where mutant IκBα was under the control of seven repeats of the tetracycline responsive element. A rabbit b globin 3' untranslated region (UTR) was inserted after IκBα to create the TRE-IκBα plasmid (Wang et al., 2010). All sequences were verified by sequencing from both ends (Genewiz). The TRE-IκBα was linearized by *Nae I* and *ApaL I* digestion. The 3.8 kb fragment containing seven TRE elements, the minimal CMV promoter, human IκBα (S32G-S36A) and the rabbit β-globin 3' UTR was purified and submitted for pronuclear injection in FVB genetic background. Positive lines were screened using human IκBα-specific primers. The selected strain was backcrossed for at least 10 times into the C57B6/J background and all experiments were done in the C57B6/J background.

Western blot analysis: Adipose tissue samples were homogenized on ice in TBS pH7.6 supplemented with HALT protease inhibitor cocktail (Thermo Scientific). This was followed by low speed centrifugation (3,000xg at 4°C), in order to remove the fat cake from the top of the tube. Thereafter, Triton X-100 detergent was added to a final concentration of 1%. The tissue homogenates were agitated for 1-2 h at 4°C, extracts were cleared at 15,000 x g for 20 minutes at 4°C and total protein concentration measured with BCA Protein Assay Kit (Pierce Protein Research Products, Thermo Scientific, USA). Equal amounts of protein from adipose tissue were mixed with 6x Laemmli sample buffer, resolved on 4-12% NuPage Bis-Tris gels (Invitrogen, USA), followed by transfer to PVDF membrane (Millipore, USA). Blots were probed with rabbit anti-mouse IkB antibodies (rabbit

polyclonal, Santa Cruz Biotechnologies, USA). Bound antibodies were detected with IRDye800-conjugated anti-rabbit secondary antibodies (Rockland). Membranes were scanned with the LI-COR Odyssey Infrared Imaging System. Adiponectin protein content was determined using a rabbit polyclonal anti mouse adiponectin antibody (Scherer et al., 1995). Actin controls were visualized with an anti-mouse actin monoclonal antibody from Cell Signaling.

Blood biochemistry: Insulin, SAA, leptin and adiponectin levels were measured by commercial ELISA kits from Millipore (Billerica, MA, USA) and anti-LPS IgG levels were measured by a commercial ELISA kit from Chondrex (Redmond, WA, USA). Glucose levels were determined with Sigma Diagnostics Glucose Reagents (Sigma, Sigma Aldrich, USA) and free fatty acids levels were measured with NEFA-HR(2) (Wako Pure Chemical Industries, Japan).

Histological analysis: Tissues were excised and fixed in 10% formalin (PBS-buffered) for 24 h. Following paraffin embedding, the tissue sections were de-paraffinized and stained with H&E, Trichrome, Picrosirius Red Stain or by immunohistochemistry. Primary antibodies were used raised against endomucin (rat monoclonal, Santa Cruz Biotechnologies, USA), BrdU (rat monoclonal, Serotec, USA), Mac2 (rat monoclonal, Cedarlane, USA) or perilipin (rabbit polyclonal, Affinity Bioreagents, Inc.) and then followed by biotinylated secondary antibodies (Dako, Glostrup, Denmark). Binding of secondary antibodies was visualized using a horseradish peroxidase- or alkaline phosphatase-coupled

streptavidin derivative and stained with DAB Chromogen A (Dako) or Red Alkaline Phosphatase substrate (Vector Laboratories) following the companies' protocols. Counterstaining was performed with hematoxylin. All the images were acquired with the Coolscope Microscope (Nikon). ImageJ was use for quantification of adipocyte size and capillary density from histological slides. In brief, images were transformed to 16-bit and the image threshold was set to selectively visualize adipocyte or endomucin positive areas prior analyses.

Isolation and differentiation of adipose stromal vascular cultures: Dissected fat tissue from two mice (4 fat pads total) were washed, minced, and then digested for two hours at 37ºC in buffer containing 100mM HEPES pH 7.4, 120mM NaCl, 50mM KCl, 5mM glucose, 1 mM $CaCl_2$, 1.5% BSA, and 1mg/mL collagenase D (Roche). Digested tissue was then filtered through a 100 μm cell strainer to remove undigested fragments. The flow-through was then centrifuged for 5 minutes at 600 x g to pellet the SV cells. The SV cells, resuspended in complete SV culture medium (DMEM/F12) (Invitrogen) plus Glutamax, Pen/Strep, and 10% FBS), were then filtered through a 40μm cell strainer to remove clumps and large adipocytes. Following centrifugation as above, SV cells were then resuspended in SV culture medium and plated onto a 6-cm tissue culture dish. For adipocyte differentiation assays, SV cells were plated onto collagen-coated dishes and grown to confluence in SV culture medium. At confluence, cells were exposed to the adipogenic cocktail containing dexamethasone (1μM), insulin (5μg/ml), isobutylmethylxanthine (0.5mM) (DMI) and rosiglitazone (1μM) in SV culture

medium. Forty-eight hours after induction, cells were maintained in SV culture medium containing insulin (5μg/ml) and rosiglitazone (1μM) until harvest.

Oil-Red O Staining: Oil-Red O staining was performed based on the manufacturers specifications. Briefly, 500mg of Oil-Red O was dissolved in 100ml of isopropanol. 60ml of this solution was mixed with 40ml of deionized water and allowed to sit at room temperature for 1 hour before filtering. Cells were washed with 1x PBS solution and fixed win 10% formalin. After 15 minutes, cells were washed twice with 1x PBS then stained for 1 hour with the Oil-Red O Solution. They were washed 4 more times with PBS, then visualized using a color scanner.

Quantitative real-time RT-PCR: Tissues were collected in RNAlater (Ambion, USA) and stored at -80°C. Trizol Reagent (Invitrogen, USA) extraction followed by RNA purification using RNeasy Mini Kit and RNase-Free DNase (Qiagen, USA). RNA was reverse transcribed to cDNA by iScript cDNA synthesis kit (Bio-Rad, USA) and IQ SYBR Green Supermix (Bio-Rad) was used for the quantitative PCR reactions. The relative expression level was calculated by the comparative Ct method using β-actin as endogenous control. Primer sequences can be found in **Table S2**.

Body composition measurements: Body composition was assessed with a Bruker Minispec mq10 whole body composition analyzer in our Metabolic Core Unit.

Metabolic chamber measurements: For the metabolic cage studies, mice were housed individually in metabolic chambers and maintained on a 12-h dark-light cycle with lights on from 7:00 a.m. to 7:00 p.m. at room temperature (20°C to 22°C). Metabolic profiles were obtained continuously using a TSE metabolic chamber system (TSE System, Germany) in an open-circuit indirect calorimetric system. All transgenic mice and their littermate controls were fed chow, HFD and water *ad libitum* as indicated.

Isolation and culture of peritoneal macrophages: The macrophages were harvested from the peritoneal cavity 5 days after an intraperitoneal injection with 2 mL 4% thioglycollate (Brewer Thioglycollate medium, Sigma, USA) in PBS solution. The macrophages were plated in high glucose DMEM supplemented with 10% FBS and left to adhere for about 3 hours. Non-adherent cells were washed away. Adherent cells were either subjected to direct RNA isolation or after LPS (Lipopolysaccharide from *E.coli 055:B5*, Sigma, USA) treatment as indicated in the Results Section.

β3-AR-agonist treatment: Intraperitoneal injections of 1 mg/kg CL316,243 with or without 10 mg/kg BrdU (Sigma, Sigma Aldrich, USA) in PBS was performed once daily for 10 days or as indicated in the Results sections.

Induction of colitis: Three rounds (day 0-6, 13-19 and 25-31) of 2% dextran sulfate sodium (DSS, MW 36000-50000, MP Biomedicals) treatment through

drinking water were performed to induce epithelial damage and colitis in RID tg and wildtype mice. DSS-treated and untreated control mice were sacrificed at day 42.

Ablation of gut microbiota: Animals were provided ampicillin (A; 1 g/kg; Sigma), vancomycin (V; 250 mg/kg; Sigma), neomycin sulfate (N; 1 g/kg; Sigma), and metronidazole (M; 1 g/kg; Sigma) as food admixes in powdered regular chow for the indicated time periods. This antibiotics supplementation was well tolerated and the mice gained weight at the same degree as untreated control.

Analysis of intestinal bacterial composition: Cecal content was collected and DNA was isolated using QIAamp DNA Stool Mini Kit (Qiagen, USA). IQ SYBR Green Supermix (Bio-Rad) was used for the quantitative PCR reactions. The relative expression level was calculated by the comparative Ct method using eubacterial 16S (amplified with universal primers, (Vaishnava et al., 2011)) as marker for total bacterial content. Primer sequences for different bacterial strains have been published previously (Deloris Alexander et al., 2006).

Co-housing experiments: Four-week-old FVB wildtype female offspring from littermate dams were co-housed with either unrelated FVB wild types or FVB RID tg females. HFD was introduced after 4 weeks and effects on glucose tolerance and hepatic steatosis were measured after and additional 7-8 weeks.

Supplemental References

Delgado-Lopez, F., and Horwitz, M.S. (2006). Adenovirus RIDalphabeta complex inhibits lipopolysaccharide signaling without altering TLR4 cell surface expression. Journal of virology *80*, 6378-6386.

Deloris Alexander, A., Orcutt, R.P., Henry, J.C., Baker, J., Jr., Bissahoyo, A.C., and Threadgill, D.W. (2006). Quantitative PCR assays for mouse enteric flora reveal strain-dependent differences in composition that are influenced by the microenvironment. Mammalian genome : official journal of the International Mammalian Genome Society *17*, 1093-1104.

Scherer, P.E., Williams, S., Fogliano, M., Baldini, G., and Lodish, H.F. (1995). A novel serum protein similar to C1q, produced exclusively in adipocytes. The Journal of biological chemistry *270*, 26746-26749.

Steed, P.M., Tansey, M.G., Zalevsky, J., Zhukovsky, E.A., Desjarlais, J.R., Szymkowski, D.E., Abbott, C., Carmichael, D., Chan, C., Cherry, L., et al. (2003). Inactivation of TNF signaling by rationally designed dominant-negative TNF variants. Science *301*, 1895-1898.

Vaishnava, S., Yamamoto, M., Severson, K.M., Ruhn, K.A., Yu, X., Koren, O., Ley, R., Wakeland, E.K., and Hooper, L.V. (2011). The antibacterial lectin RegIIIgamma promotes the spatial segregation of microbiota and host in the intestine. Science *334*, 255-258.

Wang, Z.V., Deng, Y., Wang, Q.A., Sun, K., and Scherer, P.E. (2010). Identification and characterization of a promoter cassette conferring adipocyte-specific gene expression. Endocrinology *151*, 2933-2939.

Zalevsky, J., Secher, T., Ezhevsky, S.A., Janot, L., Steed, P.M., O'Brien, C., Eivazi, A., Kung, J., Nguyen, D.H., Doberstein, S.K., et al. (2007). Dominant-negative inhibitors of soluble TNF attenuate experimental arthritis without suppressing innate immunity to infection. J Immunol *179*, 1872-1883.